

# AEROTHERMAL GROUND TESTING OF FLEXIBLE THERMAL PROTECTION SYSTEMS FOR HYPERSONIC INFLATABLE AERODYNAMIC DECELERATORS

## 9<sup>TH</sup> INTERNATIONAL PLANETARY PROBE WORKSHOP 16-22 JUNE 2012, TOULOUSE

Walter E. Bruce III<sup>(1)</sup>, Nathaniel J. Mesick<sup>(2)</sup>, Paul G. Ferlemann<sup>(3)</sup>, Paul M. Siemers III<sup>(4)</sup>, Joseph A. Del Corso<sup>(1)</sup>, Stephen J. Hughes<sup>(1)</sup>, Steven A. Tobin<sup>(5)</sup>, Matthew P. Kardell<sup>(6)</sup>

<sup>(1)</sup>NASA Langley Research Center, MS 431, Hampton, VA 23681, USA, [Walter.E.Bruce@nasa.gov](mailto:Walter.E.Bruce@nasa.gov),  
[Joseph.A.DelCorso@nasa.gov](mailto:Joseph.A.DelCorso@nasa.gov), [Stephen.J.Hughes@nasa.gov](mailto:Stephen.J.Hughes@nasa.gov)

<sup>(2)</sup> Science Systems and Applications, Inc., MS 432, Hampton, VA 23681, USA, [Nathaniel.J.Mesick@nasa.gov](mailto:Nathaniel.J.Mesick@nasa.gov)

<sup>(3)</sup> Analytical Mechanics Associates, Inc., MS 168, Hampton, VA 23681, USA, [Paul.G.Ferlemann@nasa.gov](mailto:Paul.G.Ferlemann@nasa.gov)

<sup>(4)</sup> Analytical Services and Materials, Inc., 107 Research Dr., Hampton, VA 23666, USA, [pmsswp@hctc.net](mailto:pmsswp@hctc.net)

<sup>(5)</sup> Northrop Grumman, MS 431 Hampton, VA 23681, USA, [Steven.A.Tobin@nasa.gov](mailto:Steven.A.Tobin@nasa.gov)

<sup>(6)</sup> Boeing Technology Services, 6300 J.S. McDonnell Blvd., Berkley, MO 63134, USA, [Matthew.P.Kardell@boeing.com](mailto:Matthew.P.Kardell@boeing.com)

### ABSTRACT

The Hypersonic Inflatable Aerodynamic Decelerators (HIAD) project has invested in ground tests to evaluate the aerothermal performance of various thermal protection system (TPS) candidates for use in inflatable high-drag, down-mass technology. A flexible TPS (FTPS) enables the deployment of large aeroshells which significantly reduce the ballistic coefficient of an entry vehicle allowing a greater mass to be delivered to the ground at higher landing altitude than with a conventional, rigid TPS. A HIAD requires a FTPS capable of surviving the aerothermal entry loads including heat flux, pressure, shear force, and total energy load.

Flexible TPS development involves ground testing and analysis necessary to characterize performance of the FTPS candidates prior to flight testing. This paper provides an overview of the analysis and ground testing efforts performed over the last year at the NASA Langley Research Center and in the Boeing Large-Core Arc Tunnel (LCAT). In the LCAT test series, material layups were subjected to aerothermal loads commensurate with peak re-entry conditions enveloping a range of HIAD mission trajectories. The FTPS layups were tested over a heat flux range from 20 to 50 W/cm<sup>2</sup> with associated surface pressures of 3 to 8 kPa.

To support the testing effort a significant redesign of the existing shear (wedge) model holder from previous testing efforts was undertaken to develop a new test technique for supporting and evaluating the FTPS in the high-temperature, arc jet flow. Since the FTPS test samples typically experience a geometry change during testing, computational fluid dynamic (CFD) models of the arc jet flow field and test model were developed to support the testing effort. The CFD results were used to help determine the test conditions experienced by the test samples as the surface geometry changes. This

paper includes an overview of the Boeing LCAT facility, the general approach for testing FTPS, CFD analysis methodology and results, model holder design and test methodology, and selected thermal results of several FTPS layups.

### 1. INTRODUCTION

Aerothermal ground testing is one component in the successful development of flexible thermal protection systems (FTPS) which are required for Hypersonic Inflatable Aerodynamic Decelerators (HIAD). An effort has been undertaken by NASA to develop and demonstrate operation of HIAD systems. An overview of the HIAD project is presented in [1] and overviews of the FTPS development efforts are presented in [2] and [3].

Since the development of FTPS is relatively new, there was no existing method for aerothermal testing and evaluation of these particular systems at conditions representative of HIAD mission applications when the HIAD project was initiated. Therefore, a test technique development effort was started to develop a test methodology and hardware to evaluate the FTPS under relevant flight aerothermal conditions. Over the past few years model holder hardware and test techniques have been developed and FTPS tests have been performed in the 8-Foot High Temperature Tunnel (8'HTT) at NASA Langley Research Center, the Laser Hardened Materials Evaluation Laboratory (LHMEL) at Wright-Patterson Air Force Base, and the Panel Test Facility (PTF) at NASA Ames Research Center. These testing efforts, including overviews of the facilities and selected results, are presented in [3]. Reference [3] also identified the Boeing Large Core Arc Tunnel (LCAT) as an attractive facility in terms of aerothermal performance (heat flux, surface pressure, and aerodynamic shear force) and presented predicted aerothermal performance envelopes relevant to HIAD

flight trajectories. Subsequent to the publication of [3], 8-weeks of calibration and testing have been performed in the LCAT facility as of April 2012. Hardware development, analysis, calibration, and testing have been performed for both shear (wedge) and stagnation configurations in LCAT and results of these efforts will be presented in this paper.

## 2. TEST CONDITIONS

Within the past year FTPS aerothermal testing efforts have been primarily focused on supporting aerothermal FTPS code development [3] and supporting FTPS development for the High-Energy Atmospheric Reentry Test (HEART) vehicle [4]. The code development effort is initially focused on predicting the Inflatable Reentry Vehicle Experiment-3 (IRVE-3) [3] configuration and the HEART configuration. In addition, the FTPS development effort is supporting testing and evaluation for the development of the FTPS for the HEART vehicle. Therefore, the two main flight profiles of initial interest for simulation in the LCAT facility are the HEART and IRVE-3 trajectories. A plot of stagnation point cold wall heat flux and surface pressure are shown for these two missions in Fig 1.

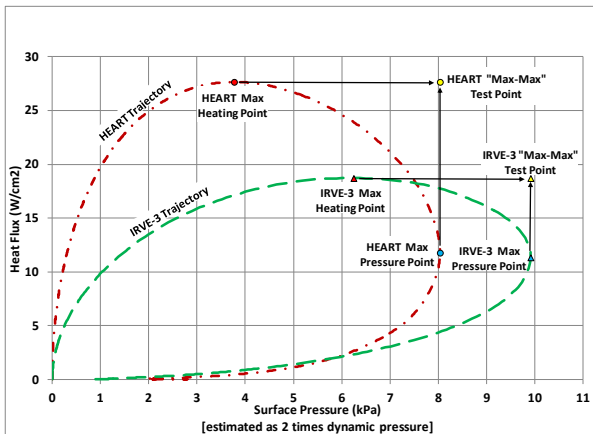


**Fig 1: Stagnation point cold wall heat flux and surface pressure for IRVE-3 and HEART flight trajectories showing various test points of interest.**

Four test conditions were calibrated in the LCAT facility for both shear and stagnation testing to provide a range of conditions for evaluating the FTPS. A wedge and a stagnation calibration probe of the same geometry as the test samples were fabricated and used to calibrate the test conditions to provide the desired heat flux and surface pressure on the samples. Slug calorimeters and pressure ports were used to determine the cold wall heat flux and the surface pressure at each condition. The four calibrated conditions are shown in Table 1. These test conditions do not match exactly the specific test points of maximum heating, maximum pressure, and the max-max test points as shown in Fig

1, but are a compromise between flight conditions for code validation, desired FTPS development conditions, and facility limitations.

Also notice that the peak heating point for the HEART trajectory is at a value of approximately  $28 \text{ W/cm}^2$ , yet test conditions have been calibrated above this heating value. The calculated trajectories show in Fig 1 are unmarginated and for a smooth wall. It is expected the FTPS will not be a smooth wall but will have geometry variations resulting from the underlying structural support, surface features such as seams and penetrations, and surface distortions resulting from wrinkles or other surface imperfections. All of these items can cause localized increased heating. Some initial calculations, presented in [4], are showing increased heating above the stagnation point calculations at the transition from the nose to inflatable region on the vehicle. In addition, the vehicle final design aerothermal conditions will be marginated to account for uncertainty and for future potential changes. In order to account for these factors, test conditions have been calibrated at higher conditions than presently calculated for the vehicle stagnation point.

**Table 1: Calibrated Cold Wall Heat Flux and Surface Pressure Conditions for Stagnation and Shear Testing**

Test Conditions	
Heat Flux (W/cm <sup>2</sup> )	Surface Pressure (kPa)
20	3.1
30	4.8
40	6.6
50	4.0

## 3. TESTING METHODOLOGY

Flight trajectories for the HEART and IRVE-3 vehicles are presented in Fig 1 with the max heating, max pressure and max-max test points identified. For screening of FTPS materials in the early stages of development a max-max test point concept was used where the arc jet test condition simultaneously simulated the maximum heating and maximum pressure the FTPS experiences during flight. This is an over-test of the FTPS and can result in false negatives, but provides a convenient method to screen multiple material systems while limiting the number of tests.

As FTPS materials are down selected to fewer systems the testing becomes more refined focusing on simulating the max heating point and the max shear points individually at the full heat load. In addition,

lower heating conditions are simulated for the maximum heat load which results in longer run times and more heat soak to the FTPS-structural support interface.

Stagnation testing results in a pure thermal evaluation of the FTPS while the shear testing evaluates the structural performance of the FTPS as a result of shear forces while subjected to the proper thermal loads. Matching the correct pressure is important for FTPS. Unlike rigid, non-porous TPS the test gas infiltrates the layers of the FTPS materials because they are porous. Testing of the individual material properties has shown that the interstitial pressure has a significant effect on the thermal conductivity of the material. Therefore, if the surface pressure is not matched during testing the FTPS will not exhibit the correct thermal transport properties. In addition, if an oxidizing material is used as the insulator the pressure and test gas are also important so the correct partial pressure of oxygen is present in the material; otherwise, the oxidation characteristics of the material will not be properly simulated.

The test techniques that have been developed and demonstrated in the LCAT facility have successfully captured the thermal performance of the material at the interface of each material layer using thermocouples. In addition, pyrometers and infrared cameras are used to measure the surface temperature and temperature distribution.

#### 4. BOEING LCAT FACILITY

The Boeing LCAT facility, located in St. Louis, MO uses a Huels arc heater and a pumped test cabin to provide the test conditions of interest as shown in Fig 2. Optical viewing ports are available for obtaining video, still pictures, and pyrometer and infrared camera thermal data. A general overview of the LCAT facility along with performance envelopes for stagnation and shear testing are presented in [5].

For stagnation testing a 15.24-cm (6-in) exit diameter, axisymmetric, conical nozzle is used to provide the correct combination of heat flux and model surface pressure. The 8.89-cm (3.5-in) diameter stagnation model is positioned on the centerline of the flow 22.86-cm (9-in) downstream of the nozzle exit so the model face can be seen through the viewing window shown in Fig 3.

For shear testing a semi-elliptic nozzle is used which has a flat bottom. The forward edge of the wedge model is positioned 0.127-cm (0.050-in) below and 0.127-cm (0.050-in) aft of the nozzle bottom as shown in Fig 4. The test sample is positioned on the wedge surface to stay within the flow-field lip disturbance from nozzle edges to provide the most uniform flow profile over the test sample. This results in a 10.16-cm

by 10.16-cm (4-in by 4-in) test sample positioned 5.08-cm (2-in) aft of the wedge leading edge.

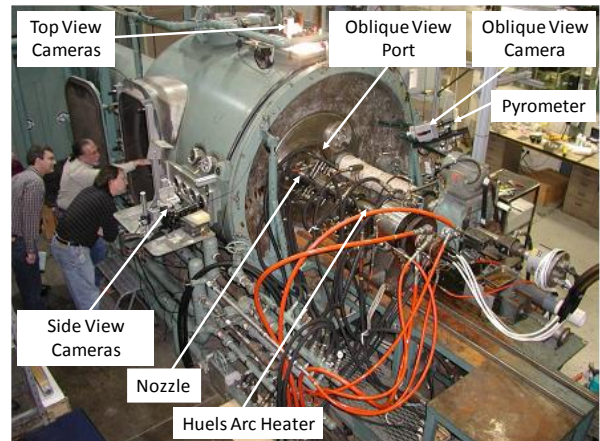


**Fig 2: View of the Boeing LCAT Facility configured for stagnation testing.**

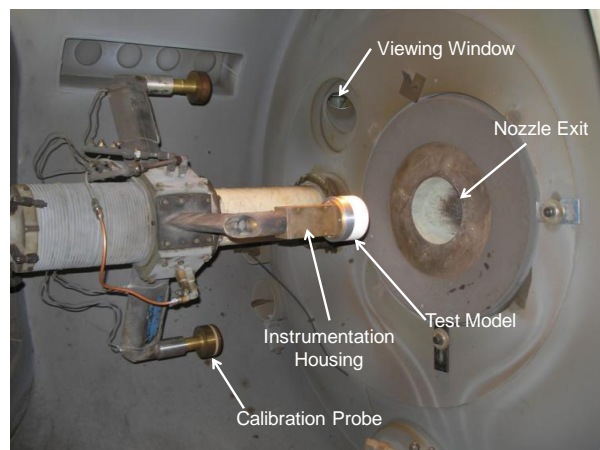


**Fig 3: View of LCAT test cabin interior and model injection system for stagnation testing.**

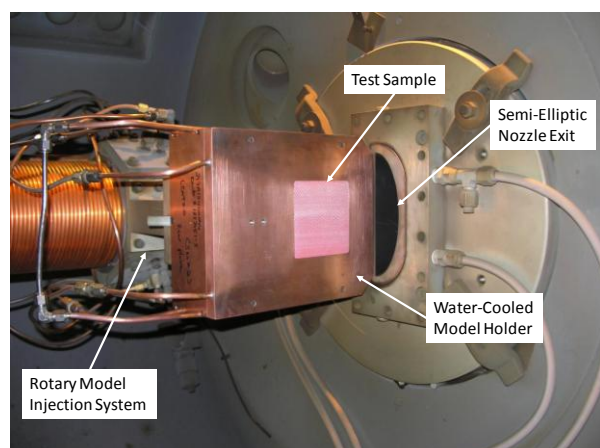


**Fig 4: View of LCAT test cabin interior and model injection system for shear testing.**

## 5. ANALYTICAL ANALYSIS

Initial shear testing in the LCAT facility showed that the test sample was not flat, but had a convex curvature of the outer surface where the center of the test sample was higher than the model holder surface. This resulted in a heating increase, as observed on the infrared camera images and post test analysis of samples, on the forward portion of the test sample. A redesign of the shear test model holder (details of the 2<sup>nd</sup> generation design are presented in Section 6) resulted in less curvature, but did not eliminate the curvature. Also, the curvature could be seen to change in height with some FTPS during the test. A computational fluid dynamic (CFD) modelling effort was undertaken to quantify the increased aerothermal conditions (heat flux, pressure, and shear) as a function of test sample curvature height. A high-level overview of the CFD effort will be presented in this paper for one specific test condition. A report presenting the comprehensive shear testing CFD analysis effort is in the review process as of the writing of this paper and will be formally published by the end of September 2012.

A 3-dimensional half-model was constructed and meshed of the semi-elliptic nozzle, starting at the converging section of the circular throat, and wedge model with the 10.16-cm by 10.16-cm (4-in by 4-in) test sample. A picture of the computational model is shown in Fig 5.

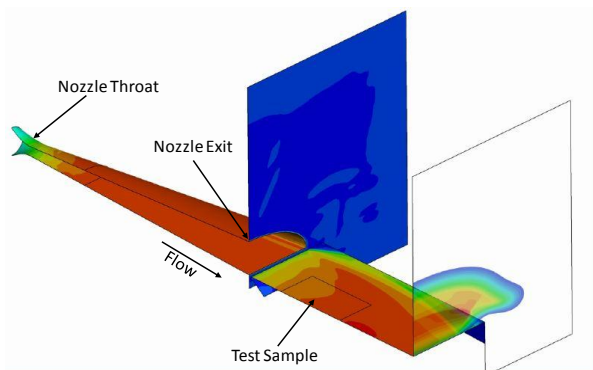


**Fig 5: CFD model of semi-elliptic nozzle and wedge test sample.**

The general process was to estimate and assign the inflow properties at the nozzle throat based on the measured arc heater conditions. The flow conditions were then calculated over a flat sample area and compared with flat plate calibration test data. The inflow conditions at the nozzle throat were adjusted until relatively close agreement was achieved between the calorimeter plate test measurements of heat flux and surface pressure and the computational values. A comparison of the flat plate heat flux calibration values and CFD results for a nominal  $20 \text{ W/cm}^2$  condition at a wedge pitch angle of  $2.5^\circ$  are shown in Fig 6.

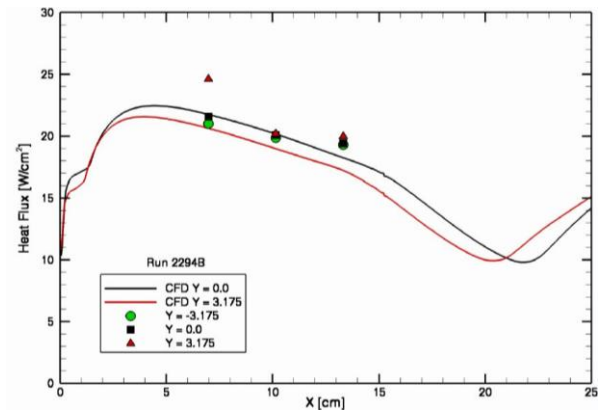


**Fig 6: CFD results (solid lines) compared with LCAT calibration data (symbols).**

Once the inflow throat conditions were established a series of parametric runs were performed at various bump heights to evaluate the heating, pressure, and shear augmentation as a function of bump height. A comparison of the flow structure in the LCAT facility, taken from screen captures from the test video, for two different bump heights and density profiles from the CFD analysis, presented in Fig 7, show that the CFD analysis is accurately capturing the flow structure over the curved test samples.

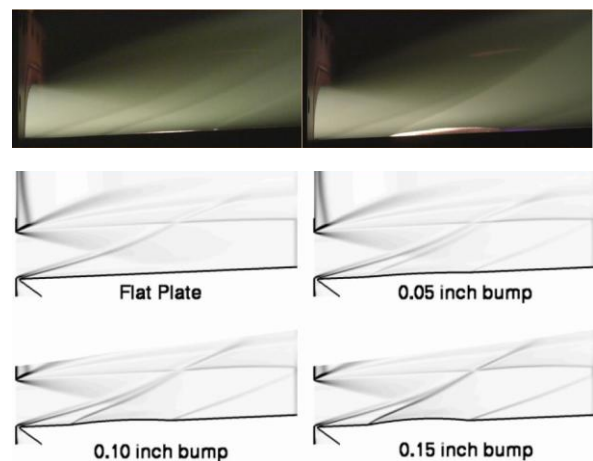


**Fig 7: Flow structure over test samples with various bump heights (pictures at top are of samples in LCAT flow, drawings are CFD results; flow is left to right).**

Heating augmentation for various bump heights are presented in Fig 8 and Fig 9 in two different formats. The CFD data shows that for a nominal  $20 \text{ W/cm}^2$  condition at the center of the test sample it is possible to have heating rates as high as  $30 \text{ W/cm}^2$  at the forward portion of the test sample with a bump height of 0.381-cm (0.15-in). However, for a smooth, uniformly curved surface, that these computations were performed on, the heating value at the center of the sample remains unchanged.

Similar results are observed for the sample surface pressure and aerodynamic shear force as shown in Fig 10 and Fig 11 respectively. Mach number, boundary layer thickness, displacement thickness, and other flow variable contours were generated as a function of bump height over the test sample and will be reported in detail in the forthcoming report.

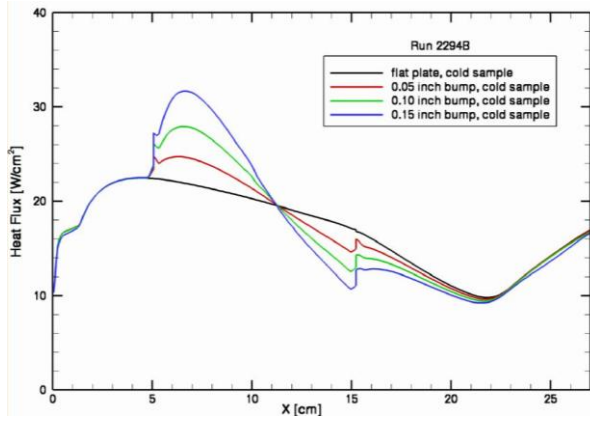


**Fig 8: CFD results showing heating augmentation for various bump heights.**

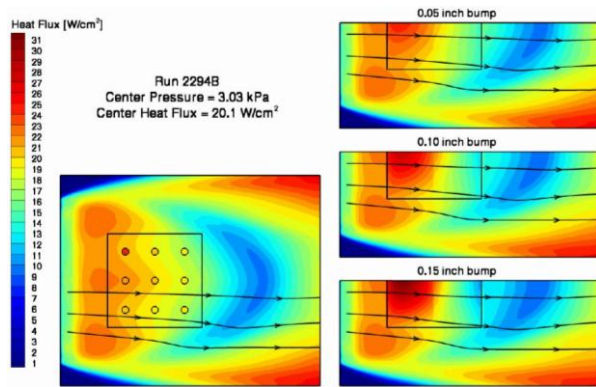


**Fig 9: CFD results showing heating augmentation for various bump heights.**

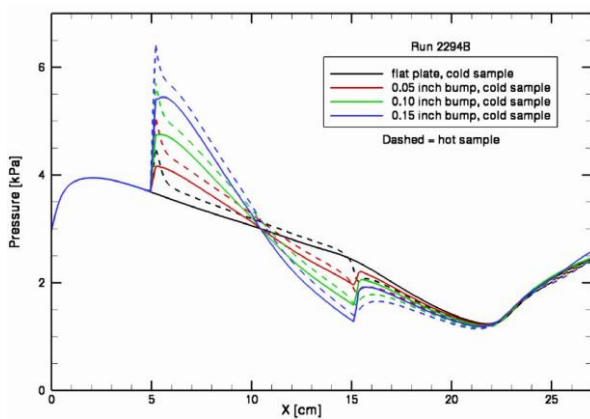


**Fig 10: CFD results showing pressure augmentation for various bump heights for cold and hot sample surfaces.**

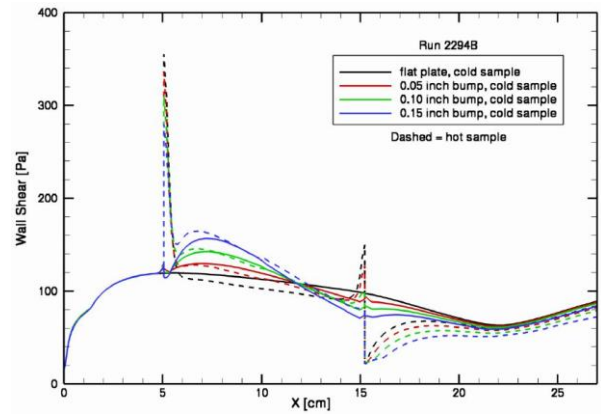


**Fig 11: CFD results showing shear force augmentation for various bump heights on cold and hot sample surfaces.**

## 6. MODEL HOLDER HARDWARE

The testing hardware serves to hold, position, and facilitate the aerothermal testing of the FTPS materials and their various configurations as a functioning FTPS. To appropriately serve this purpose the hardware must consistently hold or clamp a wide variety of candidate FTPS layups, allow placement of instrumentation at various locations throughout the FTPS, and attach to the existing test facility hardware.

### 6.1. Stagnation Fixture Hardware

The stagnation fixtures hold FTPS samples normal to the flow from an axisymmetric nozzle. Three sting arms are actuated into the flow rotationally to inject the test samples into the testing environment. A 8.89-cm (3.5-in) diameter model holder exposes a 5.72-cm (2.25-in) diameter FTPS sample face to the flow. Two model holder candidates exist: a copper water-cooled version and a passive Silicon-Carbide (SiC) coated graphite version as shown in Fig 12.



**Fig 12: Stagnation model holders prior to a test; left: copper water-cooled version, right: SiC-coated graphite version.**

The design requirements for the fixture are as follows:

1. The model holder shall passively hold or clamp a FTPS sample
  - a. The sample surface is held normal to the flow direction.

- b. The design shall accommodate a large variety of FTPS samples: firm and soft, thick and thin samples ( 0.25-cm to 1.9-cm thick).
2. The model holder shall maintain a smooth aerodynamic transition between the sample area and the model holder geometry.
3. The model holder shall consistently hold the outer fabric layers between samples.
  - a. In order to maintain repeatability between runs, two criteria should be used to maintain uniform sample geometry: pre-test tension in the outer fabric and sample curvature.
4. The model holder shall vent internal gasses without affecting the sample geometry.
5. The model holder shall be designed to mitigate hot gas inflow around or through the FTPS sample.

The stagnation model holder design is based on a 8.89-cm (3.5-in) diameter “flat face” stagnation probe geometry with a 1.27-cm (0.500-in) corner radius. The sample is exposed through a 5.72-cm (2.25-in) circular opening on the face of the model holder. To prevent an abrupt aerodynamic geometry from existing between the model holder and the sample, the model holder’s geometry tapers to a relatively thin “knife edge” at the sample area.

Three set screws adjust the placement of a backside insulator, placed behind the FTPS layup. This adjustment compensates for FTPS sample configuration and material variation. Similarly, it also controls the amount of compression placed on the FTPS insulators during the installation process. For the initial evaluation testing of the model holders, this compression is a percentage of the as-measured FTPS layer; percentages are based on the type of insulator. The adjustment range allows testing of FTPS outer fabrics only (0.102-cm or 0.040in thick) to very thick FTPS samples (~2.54-cm or ~1.00-in thick).

During the installation process, the two layers of FTPS outer fabric are frictionally held between two collars and then clamped. This process enables a consistently exposed sample geometry to be created prior to installation and compression of other FTPS layers.

Internal air must be evacuated through the sample area when the model holders are installed in the test chamber and the cabin pressure decreases prior to and during the test. This process must not adversely affect the sample geometry.

The stagnation model holders are sealed in the rear, through use of O-rings and RTV silicone. This prevents the sample from ingesting hot gas through the model holder.

Additional design features, shown in Fig 13, include instrumentation clearances, a 1.27-cm (0.50-in) thick insulator for the backside of the FTPS, and part interfaces that are tolerant of the testing temperatures.

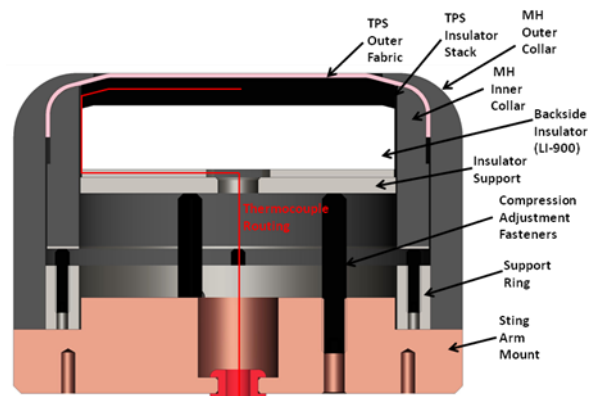


**Fig 13: Cross section of the SiC-coated graphite stagnation model holder.**

A 2-week stagnation test series was completed on 4-May-2012. This test series served to evaluate the two candidate model holder designs, obtain data for comparison to prior shear test series, and obtain a statistical data set for FTPS material performance where the focus was on variations in weight and thickness of the FTPS insulators.

Flexible TPS samples are installed into the stagnation model holders layer-by-layer. The individual layers are documented and orientations are chosen. Then, the two layers of FTPS outer fabric are clamped between the outer and inner collars. After verifying that fabric geometry is sufficient, thermocouples and other FTPS layers are added sequentially. The thermocouples are type-R in the locations closer to the exposed FTPS surface where the temperatures are higher and are type-K thermocouples elsewhere. These thermocouples are placed into the center of the sample radially, staggered at 90 degree increments as shown in Fig 14.



**Fig 14: Installation of FTPS layers and thermocouples.**

After all of the FTPS layers and instrumentation are in place, the backside insulator (fabricated from LI-900 material) is installed behind the FTPS layup and a support plate is installed as shown in Fig 15. The

support plate serves to route the instrumentation from the periphery of the insulator backside to the center of the model holder and also to prevent the FTSP compression/thickness adjustment set screws from damaging the LI-900 material.



**Fig 15: Left: backside insulator installed, right: support plate installed.**

Next, the model holder is fastened together. This is done without placing the FTSP layup in compression. With the hardware in place, the compression set screws now can be adjusted. The adjustment is based on known model holder dimensions and the individual measured FTSP layer thicknesses multiplied by compression constants. Finally, the external geometry of the FTSP sample is documented and examined with custom-made curvature gauges as shown in Fig 16.



**Fig 16: Left: hardware assembled, right: examining sample curvature.**

After the samples are assembled and installed into the stagnation model holders, the model holders are installed in the test facility.

Once the facility arc jet parameters are appropriate for the testing condition, the model holders are indexed into the flow for the appropriate length of time. During testing high-definition video and 35mm pictures (Fig 17) are made of the model.

Flexible TPS samples are typically tested until an internal temperature reaches a pre-set value, which is normally a temperature limitation placed on the outward facing side of the FTSP gas barrier.

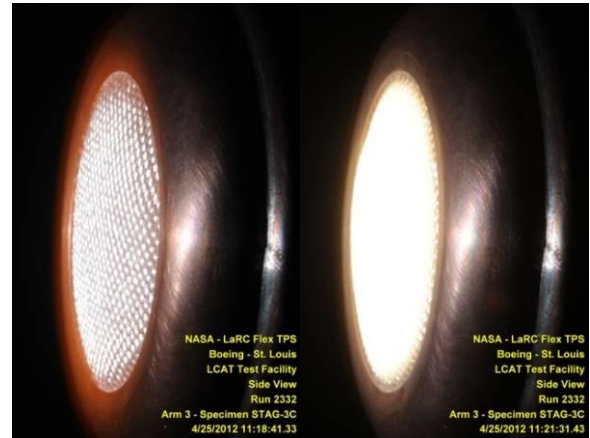


**Fig 17: Left: FTSP sample in test near the start of the test; right: FTSP sample at end of test.**

Following the test the samples are photographed prior to removal from the test sting and then after removal as shown in Fig 18.

The sample disassembly process is similar to the assembly process in reverse. The sample is uncompressed, then removed layer-by-layer. Each layer is documented with the instrumentation in place.



**Fig 18: Left: a pre-test FTSP sample; right: post test.**

Flexible TPS samples were tested in the stagnation configuration at the Boeing LCAT facility during the weeks of April 23, 2012 and April 30, 2012.

Temperature data for a FTSP sample is shown in Fig 19. This sample has seven layers; from the outermost layer they are: 2x Nextel BF-20, 4x Pyrogel 2250, and 1x Aluminized Kapton Kevlar Laminate (AKKL). This particular gas barrier (AKKL) is aluminized on one side only. This side is placed outward, facing the exposed sample area.

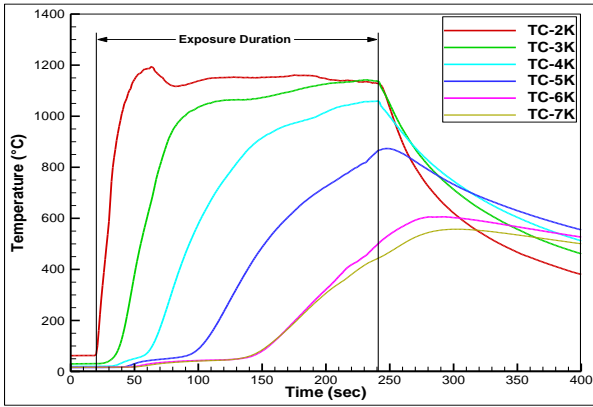


**Fig 19: Example temperature data from FTPS stagnation testing at 20W/cm<sup>2</sup> cold wall heating condition.**

The thermocouples locations are shown in Fig 20. The Pyrometer measures the surface temperature of the Nextel BF-20 outer fabric exposed surface. The pyrometer data (not show in Fig 19) is corrected for transmission losses through the test cabin window and other optics, but is not corrected for emissivity of the BF-20. The material emissivity correction is performed post-test.

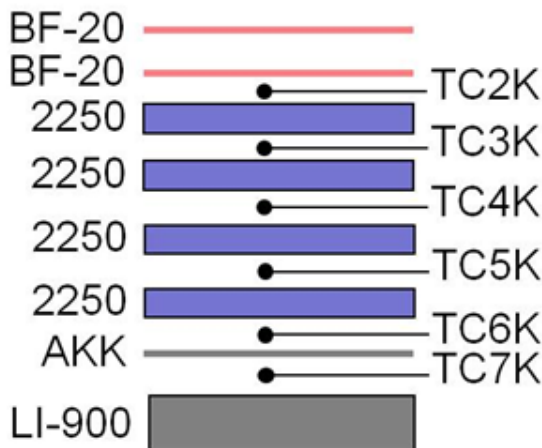


**Fig 20: Thermocouple configuration for FTPS stagnation testing.**

## 6.2. Design of the 2<sup>nd</sup> Generation Shear (Wedge-Flow) Testing Hardware

The second generation shear fixture was designed to enhance the testing capacity of FTPS materials in a shear environment. Difficulties were encountered with prior hardware; these items contributed to the requirements of the 2<sup>nd</sup> generation shear test fixture:

1. Thermal expansion of the outer fabrics of the FTPS allowed unconstrained aero-elastic response of these layers at certain test

conditions, leading to pre-mature sample failure.

2. Repeatable clamping of FTPS layups only worked consistently for thinner layups of specific thicknesses.
3. The frictional install process of pressing a sample into a cavity and clamping it made it difficult to achieve consistent and uniform tension on the FTPS outer fabric.
4. The exposed sample face geometry (protrusion distance from the cavity, sample curvature) is not optimal. The difficulty in achieving consistent aerodynamic shapes of the exposed sample face leads to uncertainty in the aerothermal heating, influencing test performance.

These items motivated a change from hardware that installed the FTPS sample by compression of the entire FTPS layup into a cavity of a fixed size to pre-tensioning the FTPS outer fabric and pre-compressing the FTPS insulators behind that fabric in a controlled, rigorous manner before installing them into the cavity that exposes the sample face to the testing environment.

The design requirements for the fixture are as follows:

1. The design shall position a sample in the arc-jet flow from a semi-elliptic nozzle.
2. The design shall contain internal mechanisms and instrumentation, to prevent damage from elevated temperatures.
3. The design shall mitigate inflow through the sample area, especially if clearances are used around the sample.
4. The model holder must have a path to evacuate the internal volume when vacuum is pulled on the test chamber.
5. The design shall have mechanisms to control these aspects of the FTPS sample geometry:
  - a. FTPS outer fabric tension
  - b. FTPS insulator compression
  - c. FTPS sample curvature
6. The design shall improve the sample profile during a test to mitigate augmented heating.
7. The design shall accommodate a wide range of FTPS layup configurations without adversely affecting their testing performance.
8. The design application shall mitigate aero-elastic response of the FTPS outer fabric.

The 2<sup>nd</sup> generation shear model holder design is based on the prior generation hardware. The primary changes between designs are related to how the sample is held in the fixture.

The model holder is a water-cooled copper enclosure that exposes the sample from a cavity in a “surface plate” that parallels the flow direction as shown in Fig



4. This enclosure is mounted to a sting arm. The angle of attack of the test surface with respect to the flow is adjustable by changing the angle of attack for the enclosure at the sting arm interface. Wedges were fabricated to allow five specific angles of attack: 0°, 2.5°, 5°, 7.5°, and 10°.

The internal mechanisms, instrumentation connectors and other lower temperature components are contained within this water-cooled enclosure. The enclosure is vented in the rear by a bleed hole, sized appropriately to not allow gross ingress of flow through the enclosure. This is done to mitigate potential damage to the hardware or unwanted thermal response at the FTPS test sample's boundary, while allowing the internal volume to evacuate during the depressurization cycle prior to a test run.

The hardware subassembly that contains the FTPS geometry control mechanisms is the "sample tensioning fixture", shown with a test sample installed in Fig 21. This assembly performs four functions: first, the FTPS sample's thickness is accommodated with adjustment fasteners; second, the same adjustment fasteners are used to compress the FTPS insulators; third, four mechanisms are used to pretension the two outer fabric layers in two directions (bi-axially); fourth, the four pretensioning mechanisms are used to actively control the FTPS test sample's external geometry in test. The functionality of the insulator compression and thickness adjustment fasteners with the outer-fabric bi-axial pretensioning allows much greater control over test surface geometry pre-test than was achieved with previous hardware for a wide range of FTPS configurations.

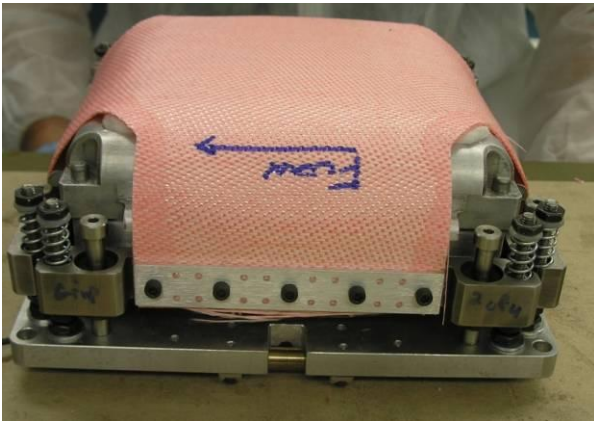


**Fig 21: The sample tensioning fixture with a FTPS sample installed.**

The sample tensioning fixture contains many design features (Fig 22) to meet aforementioned design requirements:

1. The FTPS insulators are held in an internal cavity of an outer "base ring". The cavity is sealed by an o-ring.
2. The FTPS insulators are supported on the backside by a lower base ring with a backside insulator block in the test sample area.
3. The base ring configurations contain all of the alignment geometry for the FTPS outer fabric, in order to keep the outer surface repeatable and to have reliable performance of the tensioning mechanisms in test.
4. The tensioning mechanisms clamp a 10.16-cm (4-in) long leg of the cruciform shaped outer fabric layers.
5. These tensioning mechanisms use two shoulder screws with linear bearings for translational alignment and two threaded rods with compression screws to achieve repeatable tension on the outer fabric layers.
6. A tension plate supports all four tensioning mechanisms. It aligns all of the individual subassemblies and contains attachment points for instrumentation to measure displacements at the four mechanisms.
7. Four string potentiometers are used to measure displacements; the wire rope is routed in a grooved sleeve bearing.

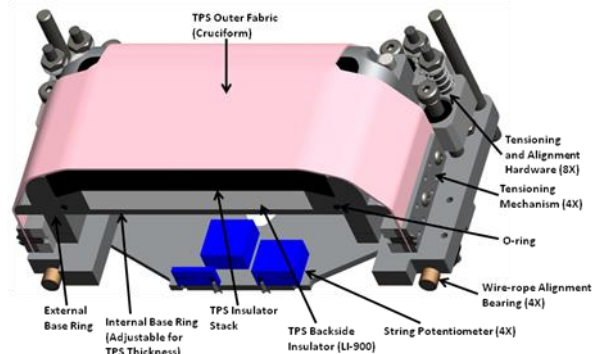


**Fig 22: Cross-section of the sample tensioning fixture.**

The grip assemblies clamp the outer fabrics mechanically with five fasteners and two "jaws". The ceramic plain bearings allow unconstrained motion parallel to the two shoulder screws' axes. The compression springs can be replaced to change amounts of tension or compressed to different displacements for fine adjustment of tension.

The assembled sample tensioning fixture with a FTPS sample is installed into the cavity in the copper water-cooled surface plate. This exposes the sample face, a 10.16-cm (4-in) square, to the testing environment.

A 2-week shear test series was completed on 17-Feb-2012. This test series served to evaluate the model holder design and obtain data for comparison to prior

shear test series with the 1<sup>st</sup> generation shear model holder.

Similar to the stagnation model holders, the samples are installed into the shear model holders layer by layer.

Each layer is placed into the sample tensioning fixture with thermocouples centrally located on the layer. The bottom layers are added first, and then built upon. After the FTPS insulation layers have been added, the cruciform shaped outer fabric layers are added. They are firmly clamped at the tensioning mechanisms and aligned before tension is placed on both layers.

The eight individual springs are compressed uniformly for the four tensioning mechanisms to achieve a uniform bi-axial tension on the FTPS outer fabric. After the outer fabric tension is set, the FTPS insulators are compressed by use of set screws (from behind the FTPS insulator cavity). During this process, the sample's external geometry is checked.

Once the FTPS geometry is appropriate, the sample tensioning fixture is attached to the surface plate by four threaded rods. The clearances at the "knife edges" are verified (Fig 23), sample protrusion height is measured, and sample curvature is documented. Alternately, the FTPS can be adjusted to clamp the sample boundary tightly. The ability to adjust the boundary conditions demonstrates the flexibility of the fixture. It also allows inspection of fixture variables that may have influence on the overall test performance of the FTPS samples.

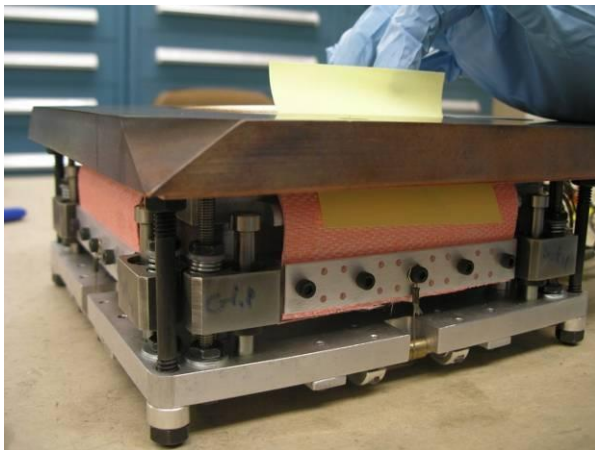


**Fig 23: Verification of clearances for the free-floating, tensioned boundary condition by freely sliding a piece of paper between the model holder knife edge and the test sample.**

The model holder is installed into the test facility after the sample preparation is complete. Similar to stagnation testing, the calibration model and FTPS test sample are rotationally indexed into appropriate flow conditions.

The test nominally concludes when an internal temperature is reached at one of the thermocouple locations. Another potential condition to retract is the gross failure of the FTPS outer fabrics during the test.

Two identical FTPS layups were tested to evaluate the effectiveness of the 2<sup>nd</sup> generation design to better constrain the FTPS sample's exposed geometry in test over the initial model holder. One layup was installed in the model holder such that it had a mechanically locked boundary condition, which is similar to the boundary condition used on the original model holder. The other sample was tested with a mechanically free-floating, actively tensioned boundary condition as intended for use with the 2<sup>nd</sup> generation fixture. The effectiveness of the new constraint system of the 2<sup>nd</sup> generation design can be seen in Fig 24 and Fig 25, which shows the differences in side profiles of the sample in the flow. Notice that the sample height is greater at the end of the run for the original constraint design (Fig 24) and has not protruded as much for the 2<sup>nd</sup> generation design (Fig 25).

The removal process for the shear samples is similar to the stagnation samples. After photo documentation of the sample in the test cell prior to removal, the sample is uncompressed, then removed layer-by-layer. Each layer is documented with photos with the instrumentation in place and notes are made of any unusual or interesting findings.



**Fig 24: Testing of a FTPS sample with a mechanically locked boundary (initial model holder design); left: beginning of run, right: end of run (flow is left to right).**



**Fig 25: Testing of a FTPS sample with a mechanically free-floating, actively tensioned boundary (2<sup>nd</sup> generation design); left: beginning of run; right: end of run (flow is left to right).**

Flexible TPS samples were tested in the shear configuration at the LCAT facility during the weeks of February 6, 2012 and February 13, 2012.

The temperature data for a FTPS sample is shown in Fig 26. This sample has five layers. From the

outermost layer they are: 2x Nextel BF-20, 1x Saffil, 1x Pyrogel 2250, and 1x Aluminized Kapton Kevlar Laminate (AKKL). This gas barrier (AKKL) is aluminized on both sides. The thermocouple locations are shown in Fig 27.

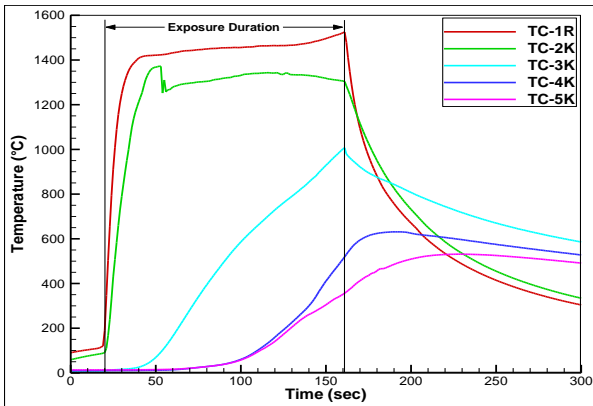


**Fig 26: Example temperature data from FTPS shear testing at 40W/cm<sup>2</sup> cold wall heating condition.**

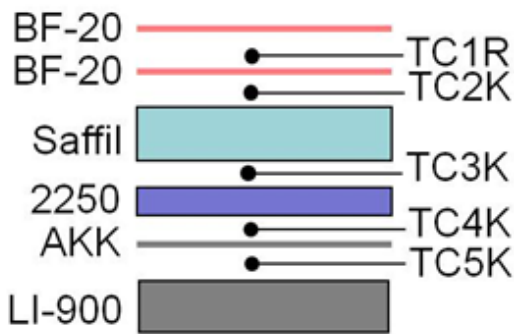


**Fig 27: Thermocouple configuration for FTPS stagnation testing.**

## 7. SUMMARY AND FUTURE PLANS

A test methodology and associated hardware have been developed for the aerothermal shear (wedge) and stagnation testing of FTPS in the Boeing LCAT facility. A second generation shear testing model holder has been designed, fabricated, and demonstrated in the LCAT facility showing improved performance for maintaining a flatter test sample profile and uniform tension in the outer FTPS layers over the original shear testing fixture.

Test conditions relevant to the IRVE-3 and HEART missions have been calibrated in the LCAT facility that result in the same pressure and heat flux conditions on the test sample in both shear and stagnation test configurations. A technique has been developed to measure the temperature as a function of time during the test at each individual layer of the FTPS using thermocouples and on the outer FTPS surface using a

pyrometer. In addition, an infrared camera is used on the shear test configuration to visualize the temperature profile over the 10.16-cm (4-in) square test sample surface.

Computational fluid dynamic analysis has been performed to evaluate flow conditions over shear (wedge) test samples and determine the sensitivity of flow parameters to bump heights. A parametric study was performed and quantified the changes in heating, pressure, shear, and other flow parameters resulting from various bump heights compared to flat plate values.

Additional testing and test technique refinement is planned to continue in the LCAT facility through fiscal year 2013. Computational fluid dynamic analysis is planned for the stagnation holders to evaluate the flow conditions over the test samples and to assist with potential improvements for a 2<sup>nd</sup> generation stagnation holder design if required. Additional instrumentation development is planned to measure the pressure between individual FTPS layers during the test. Testing will continue to support code development and the HEART vehicle. In addition, testing will be performed to evaluate new materials to improve the existing FTPS and to develop FTPS for higher heat flux applications.

## 8. REFERENCES

1. Hughes, S. J., Cheatwood, F. M., Dillman, R. A., Wright, H. S., DelCorso, J. A., Calomino, A. M., *Hypersonic Inflatable Aerodynamic Decelerator (HIAD) Technology Development Overview*, AIAA-2011-2524, May 2011.
2. DelCorso, J. A., Cheatwood, F. M., Bruce III, W. E., Hughes, S. J., and Calomino, A. M., *Advanced High-Temperature Flexible TPS for Inflatable Aerodynamic Decelerators*, AIAA-2011-2510, May 2011.
3. DelCorso, J. A., Bruce III, W. E., Hughes, S. J., Dec, J. A., Rezin, M. D., Meador, M. B., Hiaquan, G., Fletcher, D. G., Calomino, A. M., Cheatwood, F. M., *Flexible Thermal Protection System Development for Hypersonic Inflatable Aerodynamic Decelerators*, 9th International Planetary Probe Workshop, 16-22 June 2012, Toulouse, France.
4. Wright, H., Cutright, A., Corliss, J., Bruce, W., Trombetta, D., Mazaheri, A., Coleman, M., Olds, A., Hancock, S., *HEART Flight Test Overview*, 9th International Planetary Probe Workshop, 16-22 June 2012, Toulouse, France.
5. *Evaluation of the NASA Arc Jet Capabilities to Support Mission Requirements*, Office of the Chief Engineer, NASA/SP-2010-577, May 2010.